J. Fluid Mech. (1978), *vol.* 88, *part* 2, *pp.* 339–354
Printed in Great Britain

Flow in heated curved pipes

By LUN-SHIN YAO

The Rand Corporation, 1700 Main Street, Santa Monica, California 90406†

AND STANLEY A. BERGER

Department of Mechanical Engineering, University of California, Berkeley

(Received 8 November 1977)

The fully developed laminar flow in a heated curved pipe under the influence of both centrifugal and buoyancy forces is studied analytically. The pipe is assumed to be heated so as to maintain a constant axial temperature gradient. Both horizontal and vertical pipes are considered. Solutions for these two cases are obtained by regular perturbations in the Dean number and the product of the Reynolds and Rayleigh numbers; the solutions are therefore limited to small values of these parameters. Predictions of the axial and secondary flow velocities, streamlines, shear stress, temperature distribution and heat transfer are given for a representative case.

1. Introduction

Owing to its wide application in various engineering devices and a variety of physiological flow situations, both natural and artificial, the flow in a curved pipe has been extensively studied. Recently, the possibility of sodium–water fires in the secondary heat exchangers of liquid-metal fast-breeder reactors has necessitated further study of the problem with heat transfer.

We briefly review here the work in this area, both theoretical and experimental (e.g. see Eustice 1911; Taylor 1929). Dean (1927, 1928) found that flow in curved pipes can be correlated by a single non-dimensional parameter: the Dean number, which is defined as $D = 2\alpha Re^2$, where Re is the Reynolds number based on the average axial flow velocity and the radius a of the pipe and $\alpha = a/R$ is the curvature ratio of the pipe; see figures 1(*a*) and (*b*). Physically, this parameter can be considered as the ratio of the centrifugal force to the viscous force. A regular asymptotic solution was derived by Dean as a perturbation of the parabolic velocity profile in a straight tube. His analysis was restricted to small values of D.‡ This work has been extended numerically to moderate values of D using Fourier series by McConalogue & Srivastava (1968) and a finite-difference solution has been obtained by Greenspan (1973); the most recent and probably most accurate numerical solution is that of Collins & Dennis (1975). Earlier, Barua (1963) developed a crude asymptotic boundary-layer theory for large values of D. The physical reasons for the differences between the flow in curved pipes for small and large D has been clearly described in the studies of the entrance flow in curved pipes by Singh (1974) and Yao & Berger (1975) and that of the entrance flow in heated straight pipes by Yao (1977).

† Present address: Department of Mechanical and Industrial Engineering, University of Illinois, Urbana, Illinois.

‡ Dean's series solution has recently been extended by computer to 24 terms (Van Dyke 1978).

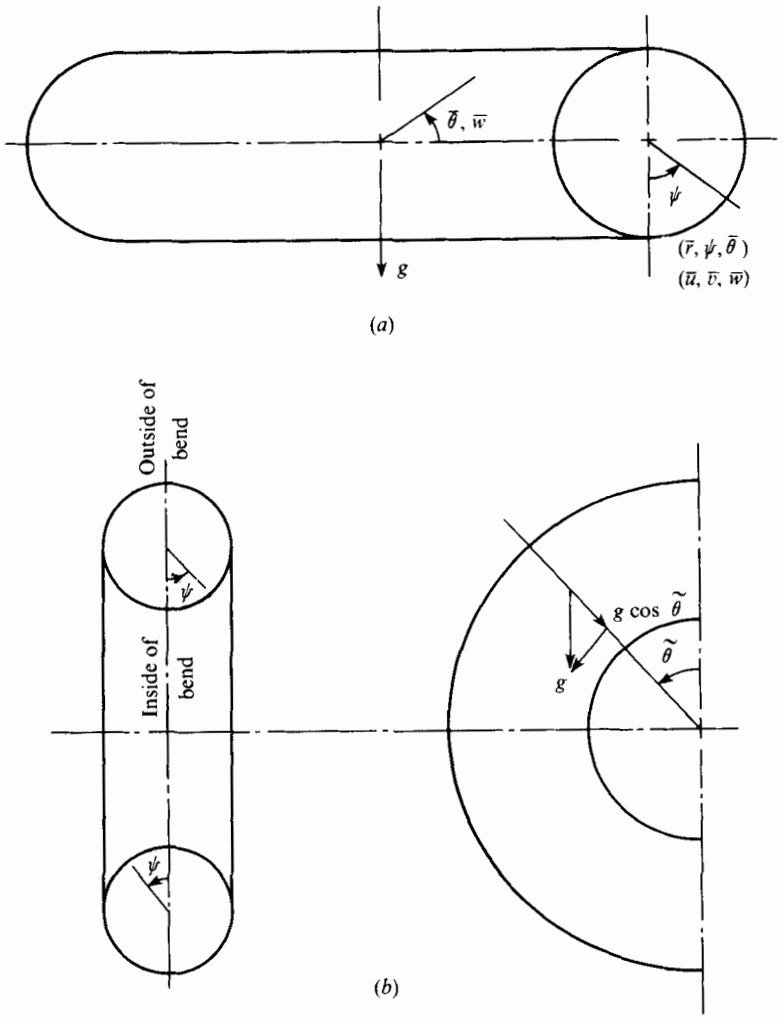

FIGURE 1. Co-ordinates for (*a*) a horizontal, (*b*) a vertical curved pipe.

Mori & Nakayama (1965) applied Barua's model of the flow to study the heat-transfer problem in a heated curved pipe. However, it has been demonstrated by Morton (1959) that the buoyancy force in a heated straight pipe can induce a secondary flow which depends on the non-dimensional parameter $ReRa$, the ratio of the buoyancy force to the viscous force, where Ra is the Rayleigh number. In the study by Mori & Nakayama (1965) the buoyancy force was neglected. This restricts their solution to cases for which D is large but $ReRa$ is very small.

In this paper, we study the flow in heated curved pipes under the influence of both centrifugal and buoyancy forces in order to gain insight into the flow pattern, local shear-stress distribution and heat-transfer mechanism, sufficiently far from the pipe entrance to avoid inlet-length effects. The pipe is heated uniformly so that a constant temperature gradient τ is maintained in the direction of the axis. Two cases are studied: a horizontal curved pipe (figure 1*a*) and a vertical curved pipe (figure 1*b*). For a horizontal curved pipe, the directions of the centrifugal force and the buoyancy force

are not coplanar and therefore the two vortices generated by the secondary flow are skewed. For a vertical curved pipe, the centrifugal force and the buoyancy force are coplanar, however it is not necessary that they be in phase.

The problem is solved by carrying out a regular perturbation in the parameters D and $ReRa$. The practical limits on the sizes of these parameters is discussed in the text. The analysis is not restricted by limits on Pr and Re; however Re must not be so large as to make the flow not laminar or to make the product $ReRa$ exceed the limit imposed.

2. Horizontal curved pipe

For a horizontal heated curved pipe whose axis is perpendicular to gravity, the governing equations of motion and energy in toroidal co-ordinates (figure 1*a*) are

$$\frac{1}{\bar{r}}\frac{\partial(\bar{r}\bar{u})}{\partial\bar{r}}+\frac{1}{\bar{r}}\frac{\partial\bar{v}}{\partial\psi}+\frac{\bar{u}\sin\psi+\bar{v}\cos\psi}{R+\bar{r}\sin\psi}=0, \tag{1a}$$

$$\bar{u}\frac{\partial\bar{u}}{\partial\bar{r}}+\frac{\bar{v}}{\bar{r}}\frac{\partial\bar{u}}{\partial\psi}-\frac{\bar{v}^2}{\bar{r}}-\frac{\bar{w}^2\sin\psi}{R+\bar{r}\sin\psi}-\beta g(T_w-T)\cos\psi$$
$$=\frac{-1}{\rho}\frac{\partial\bar{p}}{\partial\bar{r}}-\nu\left(\frac{1}{\bar{r}}\frac{\partial}{\partial\psi}+\frac{\cos\psi}{R+\bar{r}\sin\psi}\right)\left(\frac{\partial\bar{v}}{\partial\bar{r}}+\frac{\bar{v}}{\bar{r}}-\frac{1}{\bar{r}}\frac{\partial\bar{u}}{\partial\psi}\right), \tag{1b}$$

$$\bar{u}\frac{\partial\bar{v}}{\partial\bar{r}}+\frac{\bar{v}}{\bar{r}}\frac{\partial\bar{v}}{\partial\psi}+\frac{\bar{u}\bar{v}}{\bar{r}}-\frac{\bar{w}^2\cos\psi}{R+\bar{r}\sin\psi}+\beta g(T_w-T)\sin\psi$$
$$=\frac{-1}{\rho\bar{r}}\frac{\partial\bar{p}}{\partial\psi}+\nu\left(\frac{\partial}{\partial\bar{r}}+\frac{\sin\psi}{R+\bar{r}\sin\psi}\right)\left(\frac{\partial\bar{v}}{\partial\bar{r}}+\frac{\bar{v}}{\bar{r}}-\frac{1}{\bar{r}}\frac{\partial\bar{u}}{\partial\psi}\right), \tag{1c}$$

$$\bar{u}\frac{\partial\bar{w}}{\partial\bar{r}}+\frac{\bar{v}}{\bar{r}}\frac{\partial\bar{w}}{\partial\psi}+\frac{\bar{w}(\bar{u}\sin\psi+\bar{v}\cos\psi)}{R+\bar{r}\sin\psi}=\frac{-1}{\rho(R+\bar{r}\sin\psi)}\frac{\partial\bar{p}}{\partial\bar{\theta}}$$
$$+\nu\left[\left(\frac{\partial}{\partial\bar{r}}+\frac{1}{\bar{r}}\right)\left(\frac{\partial\bar{w}}{\partial\bar{r}}+\frac{\bar{w}\sin\psi}{R+\bar{r}\sin\psi}\right)+\frac{1}{\bar{r}}\frac{\partial}{\partial\psi}\left(\frac{1}{\bar{r}}\frac{\partial\bar{w}}{\partial\psi}+\frac{\bar{w}\cos\psi}{R+\bar{r}\sin\psi}\right)\right], \tag{1d}$$

$$\bar{u}\frac{\partial T}{\partial\bar{r}}+\frac{\bar{v}}{\bar{r}}\frac{\partial T}{\partial\psi}+\frac{\bar{w}}{R+\bar{r}\sin\psi}\frac{\partial T}{\partial\bar{\theta}}=\frac{\kappa}{\bar{r}(R+\bar{r}\sin\psi)}\left\{\frac{\partial}{\partial\bar{r}}\left[\bar{r}(R+\bar{r}\sin\psi)\frac{\partial T}{\partial\bar{r}}\right]\right.$$
$$\left.+\frac{\partial}{\partial\psi}\left[(R+\bar{r}\sin\psi)\frac{1}{\bar{r}}\frac{\partial T}{\partial\psi}\right]+\frac{\partial}{\partial\bar{\theta}}\left[\frac{\bar{r}}{R+\bar{r}\sin\psi}\frac{\partial T}{\partial\bar{\theta}}\right]\right\}. \tag{1e}$$

The buoyancy forces are approximated by the Boussinesq form in these equations. The fourth terms on the left-hand sides of (1*b*) and (1*c*) are centrifugal forces, which will throw the fluid particles in the core from the inside of the bend to the outside. Without the buoyancy forces, the centrifugal forces would force the secondary flow into two horizontal vortices, the line of symmetry being a horizontal line. The fifth terms on the left-hand sides of (1*b*) and (1*c*) are the buoyancy forces, which will make the fluid in the core move downwards and lead to two vertical vortices. Thus the combination of the centrifugal forces and the buoyancy forces generates two vortices whose line of symmetry intersects the direction of gravity at a finite angle. Also, the line of symmetry is no longer a straight line when both body forces act on the fluid

particles. When $ReRa$ and D are small the length scale necessary for flow in a heated curved pipe to become fully developed is aRe, the same as for an unheated straight pipe. We now introduce the following non-dimensional variables:

$$\left.\begin{aligned} &\bar{r} = ar, \quad R\bar{\theta} = (aRe)\,\theta \quad \text{(co-ordinates)},\\ &\bar{w} = W_c w, \quad \bar{u} = (\nu/a)\,u, \quad \bar{v} = (\nu/a)\,v \quad \text{(velocities)},\\ &\bar{p} = \rho W_c^2 p \quad \text{(pressure)},\\ &T = T_w - \tau a Pr\,\Theta(r,\psi), \quad T_w = T_0 + \tau(R\bar{\theta}) \quad \text{(temperature)},\\ &D = 2\alpha Re^2, \quad Ra = (\beta g a^4 \tau/\nu^2)\,Pr, \quad Re = W_c a/\nu, \end{aligned}\right\} \tag{2}$$

where a is the radius of the pipe, τ is the temperature gradient along the pipe, Pr is the Prandtl number, W_c is the velocity at $r = 0$, T_w is the wall temperature, T_0 is the reference wall temperature, β is the thermal expansion coefficient and ν is the kinematic viscosity. Substituting (2) into (1), neglecting terms $O(\alpha)$ and smaller, and eliminating the pressure terms between (1 b, c) by cross-differentation gives the following set of equations:

$$\nabla_1^4 f - \frac{1}{r}\frac{\partial(f,\nabla_1^2 f)}{\partial(r,\psi)} - \frac{1}{r^2}\frac{\partial f}{\partial \psi}\nabla_1^2 f = Ra\left(\frac{\partial \Theta}{\partial r}\sin\psi + \frac{1}{r}\frac{\partial \Theta}{\partial \psi}\cos\psi\right) - \frac{D}{2}\left(\frac{\partial w^2}{\partial r}\cos\psi - \frac{1}{r}\frac{\partial w^2}{\partial \psi}\sin\psi\right), \tag{3a}$$

$$\nabla_1^2 w + 4 = \frac{1}{r}\frac{\partial(f,w)}{\partial(r,\psi)}, \tag{3b}$$

$$\nabla_1^2 \Theta + Re\, w = \frac{Pr}{r}\frac{\partial(f,\Theta)}{\partial(r,\psi)}, \tag{3c}$$

where

$$-\frac{\partial p}{\partial \theta} = 4, \quad \nabla_1^2 = \frac{\partial^2}{\partial r^2} + \frac{1}{r}\frac{\partial}{\partial r} + \frac{1}{r^2}\frac{\partial^2}{\partial \psi^2},$$

$$\frac{\partial(A,B)}{\partial(r,\psi)} = \frac{\partial A}{\partial r}\frac{\partial B}{\partial \psi} - \frac{\partial A}{\partial \psi}\frac{\partial B}{\partial r}$$

and f is the non-dimensional stream function, defined by

$$u = -r^{-1}\,\partial f/\partial \psi, \quad v = \partial f/\partial r. \tag{3d}$$

The appearance of the factor Re in the second term of (3 c) simply reflects the fact that the wall temperature rises linearly on a length scale aRe, which is the distance over which the flow becomes fully developed.

The boundary conditions are

$$\left.\begin{aligned} &u, v, w, \Theta = 0 \quad \text{at} \quad r = 1,\\ &u, v, w, \Theta \quad \text{finite at} \quad r = 0. \end{aligned}\right\} \tag{4}$$

Although solution of (3) subject to (4) is a matter of considerable difficulty, successive approximations to the solution can be determined by expanding w, f and Θ as power

series in the Rayleigh number and the Dean number when both are small. Accordingly, suppose that

$$\left.\begin{aligned} w &= w_0 + (Raw_{10} + Dw_{11}) + (Ra^2 w_{20} + RaDw_{21} + D^2 w_{22}) + \ldots, \\ f &= \quad\quad (Raf_{10} + Df_{11}) \;\; + (Ra^2 f_{20} \;\; + RaDf_{21} + \;\; D^2 f_{22}) + \ldots, \\ \Theta &= \Theta_0 + (Ra\Theta_{10} + D\Theta_{11}) + (Ra^2\Theta_{20} + RaD\Theta_{21} + D^2\Theta_{22}) + \ldots, \end{aligned}\right\} \tag{5}$$

noting that the leading term f_0 must vanish because there is no circulation when Ra and D are zero.

Substitution of (5) into (3) and collection of terms of equal order gives:

$$\nabla_1^2 w_0 + 4 = 0, \quad \nabla_1^2 \Theta_0 + Rew_0 = 0 \tag{6a,b}$$

from terms of order zero;

$$\nabla_1^4 f_{10} = \left(\sin\psi \frac{\partial}{\partial r} + \frac{\cos\psi}{r}\frac{\partial}{\partial\psi}\right)\Theta_{,,} \tag{7a}$$

$$\nabla_1^2 w_{10} = \frac{1}{r}\frac{\partial(f_{10}, w_0)}{\partial(r,\psi)}, \tag{7b}$$

$$\nabla_1^2 \Theta_{10} + Rew_{10} = \frac{Pr}{r}\frac{\partial(f_{10}, \Theta_0)}{\partial(r,\psi)} \tag{7c}$$

from terms of order Ra;

$$\nabla_1^4 f_{11} = \left(-\cos\psi \frac{\partial}{\partial r} + \frac{\sin\psi}{r}\frac{\partial}{\partial\psi}\right)\frac{w_0^2}{2}, \tag{8a}$$

$$\nabla_1^2 w_{11} = \frac{1}{r}\frac{\partial(f_{11}, w_0)}{\partial(r,\psi)}, \tag{8b}$$

$$\nabla_1^2 \Theta_{11} + Re\, w_{11} = \frac{Pr}{r}\frac{\partial(f_{11}, \Theta_0)}{\partial(r,\psi)} \tag{8c}$$

from terms of order D;

$$\nabla_1^4 f_{20} = \frac{1}{r}\frac{\partial(f_{10}, \nabla_1^2 f_{10})}{\partial(r,\psi)} + \frac{1}{r^2}\frac{\partial f_{10}}{\partial\psi}\nabla_1^2 f_{10} + \left(\sin\psi\frac{\partial}{\partial r} + \frac{\cos\psi}{r}\frac{\partial}{\partial\psi}\right)\Theta_{10}, \tag{9a}$$

$$\nabla_1^2 w_{20} = \frac{1}{r}\left[\frac{\partial(f_{10}, w_{10})}{\partial(r,\psi)} - \frac{\partial(f_{20}, w_0)}{\partial(r,\psi)}\right], \tag{9b}$$

$$\nabla_1^2 \Theta_{20} + Rew_{20} = \frac{Pr}{r}\left[\frac{\partial(f_{10}, \Theta_{10})}{\partial(r,\psi)} - \frac{\partial(f_{20}, \Theta_0)}{\partial(r,\psi)}\right] \tag{9c}$$

from terms of order Ra^2;

$$\begin{aligned} \nabla_1^4 f_{21} = {} & \frac{1}{r}\left[\frac{\partial(f_{10}, \nabla_1^2 f_{11})}{\partial(r,\psi)} + \frac{\partial(f_{11}, \nabla_1^2 f_{10})}{\partial(r,\psi)}\right] + \frac{1}{r^2}\left[\frac{\partial f_{11}}{\partial\psi}\nabla_1^2 f_{10} + \frac{\partial f_{10}}{\partial\psi}\nabla_1^2 f_{11}\right] \\ & + \left[\sin\psi\frac{\partial}{\partial r} + \frac{\cos\psi}{r}\frac{\partial}{\partial\psi}\right]\Theta_{11} + \left[-\cos\psi\frac{\partial}{\partial r} + \frac{\sin\psi}{r}\frac{\partial}{\partial\psi}\right] w_0 w_{10}, \end{aligned} \tag{10a}$$

$$\nabla_1^2 w_{21} = \frac{1}{r}\left[\frac{\partial(f_{10}, w_{11})}{\partial(r,\psi)} - \frac{\partial(f_{11}, w_{10})}{\partial(r,\psi)}\right], \tag{10b}$$

$$\nabla_1^2 \Theta_{21} + Re\, w_{21} = \frac{Pr}{r}\left[\frac{\partial(f_{10}, \Theta_{11})}{\partial(r, \psi)} - \frac{\partial(f_{11}, \Theta_{10})}{\partial(r, \psi)}\right] \tag{10c}$$

from terms of order RaD;

$$\nabla_1^4 f_{22} = \frac{1}{r}\frac{\partial(f_{11}, \nabla_1^2 f_{11})}{\partial(r, \psi)} + \left[-\cos\psi\frac{\partial}{\partial\psi} + \frac{\sin\psi}{r}\frac{\partial}{\partial\psi}\right] w_0 w_{11}, \tag{11a}$$

$$\nabla_1^2 w_{22} = \frac{1}{r}\frac{\partial(f_{11}, w_{11})}{\partial(r, \psi)} - \frac{\partial(f_{22}, w_0)}{\partial(r, \psi)}, \tag{11b}$$

$$\nabla_1^2 \Theta_{22} + Re w_{22} = \frac{Pr}{r}\frac{\partial(f_{11}, \Theta_{11})}{\partial(r, \psi)} - \frac{\partial(f_{22}, \Theta_0)}{\partial(r, \psi)} \tag{11c}$$

from terms of order D^2.

Equations (6) are those for a fully developed straight flow without density stratification. Equations (10) represent the effects of the interaction of the centrifugal forces and the buoyancy forces. Equations of still higher orders can be obtained systematically as outlined above. The solutions of the above equations satisfying (4) can be determined straightforwardly by the method of separation of variables. The effect of the centrifugal force, as demonstrated by Dean (1928), and the effect of the buoyancy force, as illustrated by Morton (1959), on the total flux and heat transfer can be ignored to first order: these effects first start to show up in the second-order approximation. However, the solutions of these authors are limited to the cases when D or $ReRa$ is small, therefore their correlations have limited practicality. For the purpose of studying flow patterns, local heat transfer and shear stress the solutions obtained from the first-order approximation are sufficient, and the results will be valuable in gaining insight into the problem and for future studies of the flow when D and $ReRa$ are large. The three-term series solutions for the first-order approximation are presented below.

The solution of (6)–(8) satisfying (4) can be written in separable form as

$$w = w_0(r) + ReRa\bar{w}_{10}(r)\cos\psi + D\bar{w}_{11}(r)\sin\psi, \tag{12a}$$

$$f = ReRa\bar{f}_{10}(r)\sin\psi + D\bar{f}_{11}(r)\cos\psi, \tag{12b}$$

$$\Theta = \Theta_0(r) + ReRa\bar{\Theta}_{10}(r)\cos\psi + D\bar{\Theta}_{11}(r)\sin\psi. \tag{12c}$$

The equations governing the r-dependent functions in (12) are obtained in the usual straightforward manner and we do not bother to list them here. Their solutions can be obtained simply and are as follows:

$$w_0 = 1 - r^2, \quad \Theta_0 = \frac{Re}{16}(1 - r^2)(3 - r^2); \tag{13a}$$

$$\left.\begin{aligned}
\bar{f}_{10}(r) &= \frac{1}{4608} r(1-r^2)^2(10-r^2) = \frac{1}{4608}(10r - 21r^3 + 12r^5 - r^7),\\
\bar{w}_{10}(r) &= \frac{1}{184320} r(1-r^2)(49 - 51r^2 + 19r^4 - r^6),\\
\bar{\Theta}_{10}(r) &= \frac{Re}{22118400}[(381 + 1325Pr)r - (735 + 3000Pr)r^3 + (500 + 2600Pr)r^5\\
&\quad - (175 + 1125Pr)r^7 + (30 + 202Pr)r^9 - (1 + 2Pr)r^{11}];
\end{aligned}\right\} \tag{13b}$$

$$\left.\begin{aligned}
\bar{f}_{11}(r) &= \frac{1}{576} r(1-r^2)^2(4-r^2) = \frac{1}{576}(4r - 9r^3 + 6r^5 - r^7),\\
\bar{w}_{11}(r) &= \frac{1}{23040} r(1-r^2)(19 - 21r^2 + 9r^4 - r^6),\\
\bar{\Theta}_{11}(r) &= \frac{Re}{23040}[(1{\cdot}2166 + 4{\cdot}2916Pr)\, r - (2{\cdot}375 + 10Pr)\, r^3\\
&\quad + (1{\cdot}6667 + 9{\cdot}1667Pr)\, r^5 - (0{\cdot}625 + 4{\cdot}375Pr)\, r^7 + (0{\cdot}125 + Pr)\, r^9\\
&\quad - (0{\cdot}0083 + 0{\cdot}083Pr)\, r^{11}].
\end{aligned}\right\} \tag{13c}$$

3. Vertical curved pipe

The directions of the centrifugal forces and the buoyancy forces are coplanar in this case, however the magnitude of the buoyancy forces varies as $\cos\tilde{\theta}$ (figure 1*b*). Therefore fully developed flow in a heated vertical curved pipe varies periodically; its periodicity is 2π, coinciding with the periodicity of the cosine function. Referring to figure 1(*b*), the equations of motion can be expressed as

$$\frac{1}{\bar{r}}\frac{\partial(\bar{r}\bar{u})}{\partial\bar{r}} + \frac{1}{\bar{r}}\frac{\partial\bar{v}}{\partial\psi} + \frac{\bar{v}\sin\psi - \bar{u}\cos\psi}{R - \bar{r}\cos\psi} = 0, \tag{14a}$$

$$\begin{aligned}
\bar{u}\frac{\partial\bar{u}}{\partial\bar{r}} + \frac{\bar{v}}{\bar{r}}\frac{\partial\bar{u}}{\partial\psi} - \frac{\bar{v}^2}{\bar{r}} + \frac{\bar{w}^2\cos\psi}{R - \bar{r}\cos\psi} - \beta g(T_w - T)\cos\psi\cos\tilde{\theta}\\
= \frac{-1}{\rho}\frac{\partial\bar{p}}{\partial\bar{r}} + \nu\left[-\left(\frac{1}{\bar{r}}\frac{\partial}{\partial\psi} + \frac{\sin\psi}{R - \bar{r}\cos\psi}\right)\left(\frac{\partial\bar{v}}{\partial\bar{r}} + \frac{\bar{v}}{\bar{r}} - \frac{1}{\bar{r}}\frac{\partial\bar{u}}{\partial\psi}\right)\right],
\end{aligned} \tag{14b}$$

$$\begin{aligned}
\bar{u}\frac{\partial\bar{v}}{\partial\bar{r}} + \frac{\bar{v}}{\bar{r}}\frac{\partial\bar{v}}{\partial\psi} + \frac{\bar{u}\bar{v}}{\bar{r}} - \frac{\bar{w}^2\sin\psi}{R - \bar{r}\cos\psi} + \beta g(T_w - T)\sin\psi\cos\tilde{\theta}\\
= \frac{-1}{\rho\bar{r}}\frac{\partial\bar{p}}{\partial\psi} + \nu\left[\left(\frac{\partial}{\partial\bar{r}} - \frac{\cos\psi}{R - \bar{r}\sin\psi}\right)\left(\frac{\partial\bar{v}}{\partial\bar{r}} + \frac{\bar{v}}{\bar{r}} - \frac{1}{\bar{r}}\frac{\partial\bar{u}}{\partial\psi}\right)\right],
\end{aligned} \tag{14c}$$

$$\begin{aligned}
\bar{u}\frac{\partial\bar{w}}{\partial\bar{r}} + \frac{\bar{v}}{\bar{r}}\frac{\partial\bar{w}}{\partial\psi} + \frac{\bar{w}(\bar{v}\sin\psi - \bar{u}\cos\psi)}{R - \bar{r}\cos\psi} - \beta g(T_w - T)\sin\tilde{\theta}\\
= \frac{-1}{\rho(R - \bar{r}\cos\psi)}\frac{\partial\bar{p}}{\partial\tilde{\theta}} + \nu\left[\left(\frac{\partial}{\partial\bar{r}} + \frac{1}{\bar{r}}\right)\left(\frac{\partial\bar{w}}{\partial\bar{r}} - \frac{\bar{w}\cos\psi}{R - \bar{r}\cos\psi}\right)\right.\\
\left. + \frac{1}{\bar{r}}\frac{\partial}{\partial\psi}\left(\frac{1}{\bar{r}}\frac{\partial\bar{w}}{\partial\psi} - \frac{\bar{w}\sin\psi}{R - \bar{r}\cos\psi}\right)\right],
\end{aligned} \tag{14d}$$

$$\begin{aligned}
\bar{u}\frac{\partial T}{\partial r} + \frac{\bar{v}}{\bar{r}}\frac{\partial T}{\partial\psi} + \frac{\bar{w}}{R - \bar{r}\cos\psi}\frac{\partial T}{\partial\tilde{\theta}}\\
= \frac{\kappa}{\bar{r}(R - \bar{r}\cos\psi)}\left[\frac{\partial}{\partial\bar{r}}\left[\bar{r}(R - \bar{r}\cos\psi)\frac{\partial T}{\partial\bar{r}}\right] + \frac{\partial}{\partial\psi}\left[\frac{(R - \bar{r}\cos\psi)}{\bar{r}}\frac{\partial T}{\partial\psi}\right]\right],
\end{aligned} \tag{14e}$$

where $\tilde{\theta}$ is the angle measured from the upward vertical.

The non-dimensional variables are similar to the ones used for the flow in a horizontal pipe. However, the length scale along the axis of the pipe is

$$R\tilde{\theta} = aRe\theta + R\tilde{\theta}. \tag{15}$$

This equation is an expression of the physical fact that the flow becomes fully developed at a distance $O(aRe)$ from the entrance of the pipe and that local flow changes due to

the periodic buoyancy forces are based on the reciprocal of the curvature of the curved pipe. By the definition of fully developed flow, the dependence of the flow on $\tilde{\theta}$ should be diminished. It can be shown that the dependence on $\tilde{\theta}$ is of higher order, $O(\alpha Re)$, and can be neglected when D and $ReRa$ are small. In other words, the flow varies in phase with the buoyancy forces. Substitution of the non-dimensional variables given in (2) and (15) into (14) and elimination of the pressure terms between (14*b*, *c*) yields

$$\nabla_1^4 f - \frac{1}{r}\frac{\partial(f, \nabla_1^2 f)}{\partial(r, \psi)} - \frac{1}{r^2}\frac{\partial f}{\partial \psi}\nabla_1^2 f = Ra\left(\sin\psi\frac{\partial}{\partial r} + \frac{\cos\psi}{r}\frac{\partial}{\partial\psi}\right)\Theta\cos\tilde{\theta} - D\left(\sin\psi\frac{\partial}{\partial r} + \frac{\cos\psi}{r}\frac{\partial}{\partial\psi}\right)w^2, \tag{16a}$$

$$\nabla_1^2 w + 4 = \frac{1}{r}\frac{\partial(f, w)}{\partial(r, \psi)}, \quad \nabla_1^2\Theta + Rew = \frac{Pr}{r}\frac{\partial(f, \Theta)}{\partial(r, \psi)}. \tag{16b, c}$$

The perturbation equations are obtained by substituting the series (5) into (16) and up to first order are

$$\nabla_1^2 w_0 + 4 = 0, \quad \nabla_1^2\Theta + Rew_0 = 0; \tag{6a, b}$$

$$\nabla_1^4 f_{10} = \left(\sin\psi\frac{\partial}{\partial r} + \frac{\cos\psi}{r}\frac{\partial}{\partial\psi}\right)\Theta_0\cos\tilde{\theta}, \tag{17a}$$

$$\nabla_1^2 w_{10} = \frac{1}{r}\frac{\partial(f_{10}, w_0)}{\partial(r, \psi)}, \tag{17b}$$

$$\nabla_1^2\Theta_{10} + Rew_{10} = \frac{Pr}{r}\frac{\partial(f_{10}, \Theta_0)}{\partial(r, \psi)}. \tag{17c}$$

The solutions which satisfy (4) can be expressed as

$$w = w_0 + [ReRa\bar{w}_{10}(r)\cos\tilde{\theta} - D\bar{\bar{w}}_{11}(r)]\cos\psi + \ldots, \tag{18a}$$

$$f = -[ReRa\bar{f}_{10}(r)\cos\tilde{\theta} - D\bar{\bar{f}}_{11}(r)]\sin\psi + \ldots, \tag{18b}$$

$$\Theta = \Theta_0 + [ReRa\bar{\Theta}_{10}(r)\cos\tilde{\theta} - D\bar{\bar{\Theta}}_{11}(r)]\cos\psi + \ldots, \tag{18c}$$

where the barred functions on the right-hand sides are the same as in (13). The solutions (18) show that the buoyancy forces enhance the effect of the centrifugal forces along the lower half of the curved pipe ($90° \leqslant \tilde{\theta} \leqslant 270°$) and reduce the effect of the centrifugal forces along the upper half ($-90° \leqslant \tilde{\theta} \leqslant 90°$).

4. Results and discussion

The solutions presented for horizontal and vertical curved pipes are nominally limited to the cases when D and $ReRa$ are both small. A comparison by Dean (1928) of various terms in his perturbation solution for a curved pipe and a similar comparison by Morton (1959) for a heated pipe suggest that the present solution should be valid for $D \lesssim 500$ and $ReRa \lesssim 3000$. The results presented below are for the representative case $D = 300$ and $ReRa = 1000$. (The solution is valid for arbitrary Pr. In the representative case we use the value $Pr = 1$.)

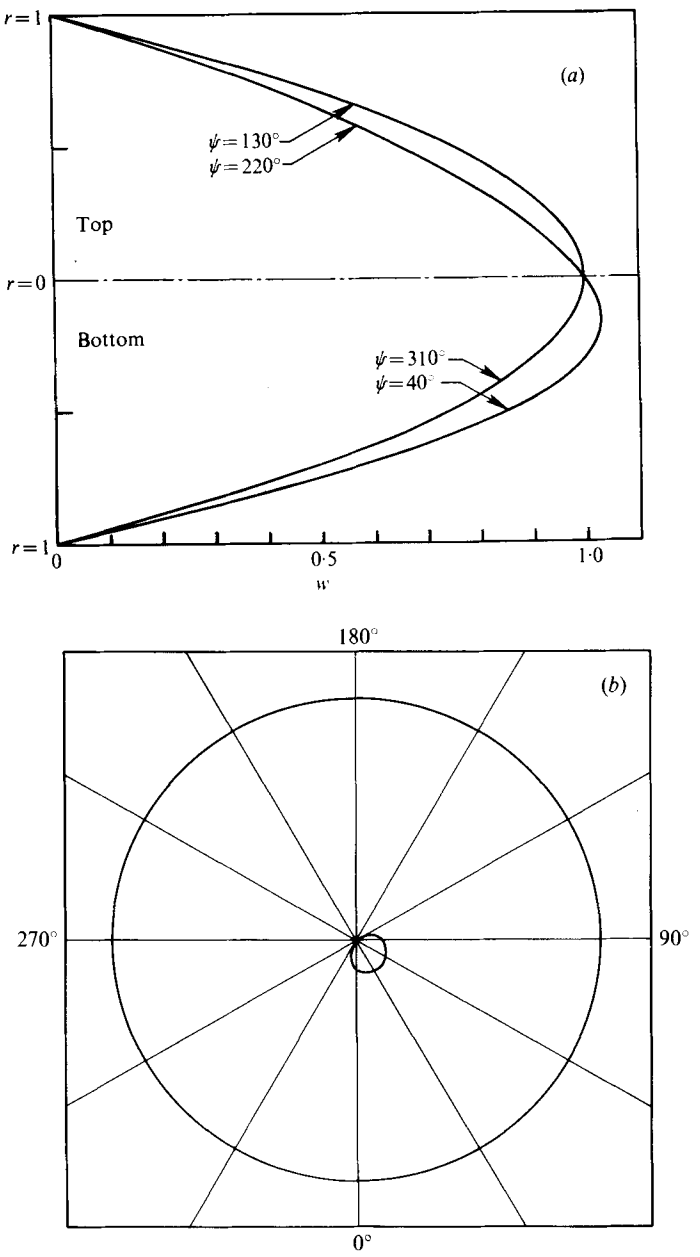

FIGURE 2. (*a*) Axial velocity profiles and (*b*) contour of maximum axial velocity for a horizontal curved pipe ($ReRa$ = 1000, D = 300).

Axial velocity

The axial velocity profiles w in the horizontal curved pipe are given in figure 2(*a*). The point of maximum axial velocity is displaced from the central axis of the pipe and occurs at approximately $\psi = 40°$, $r = 0{\cdot}25$. In figure 2(*b*) the contour of the maximum axial velocity is symmetric about the line 40°–220°, which indicates that the dividing streamline of the two vortices will lie in the neighbourhood of this line.

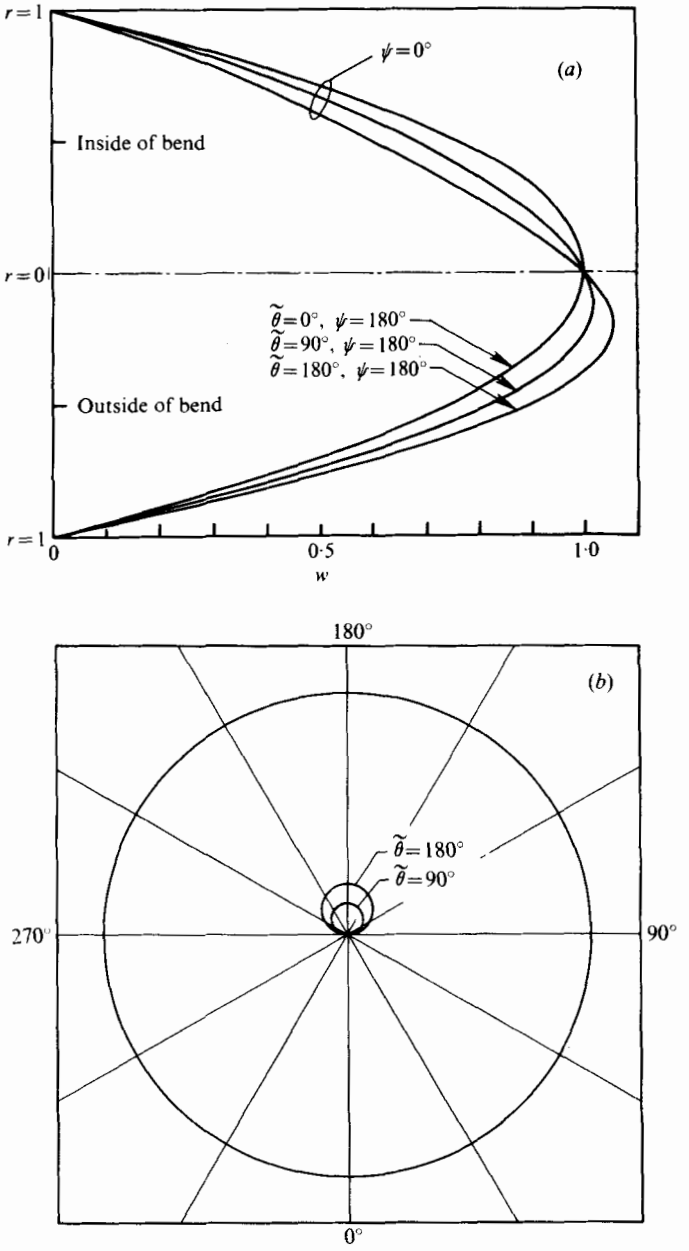

FIGURE 3. (*a*) Axial velocity profiles and (*b*) contour of maximum axial velocity for a vertical curved pipe ($ReRa$ = 1000, D = 300).

A similar plot of the axial velocity profiles in the vertical curved pipe is given in figure 3 (*a*). At the top of the curved pipe ($\tilde{\theta}$ = 0°), the axial velocity profile deviates only slightly from the Poiseuille profile. This is because of the opposing effects of the buoyancy force and the centrifugal force. The maximum velocity point will move towards the outside of the bend (ψ = 180°) when the magnitude of the buoyancy force is less than the centrifugal force and towards the inside of the bend when the buoyancy

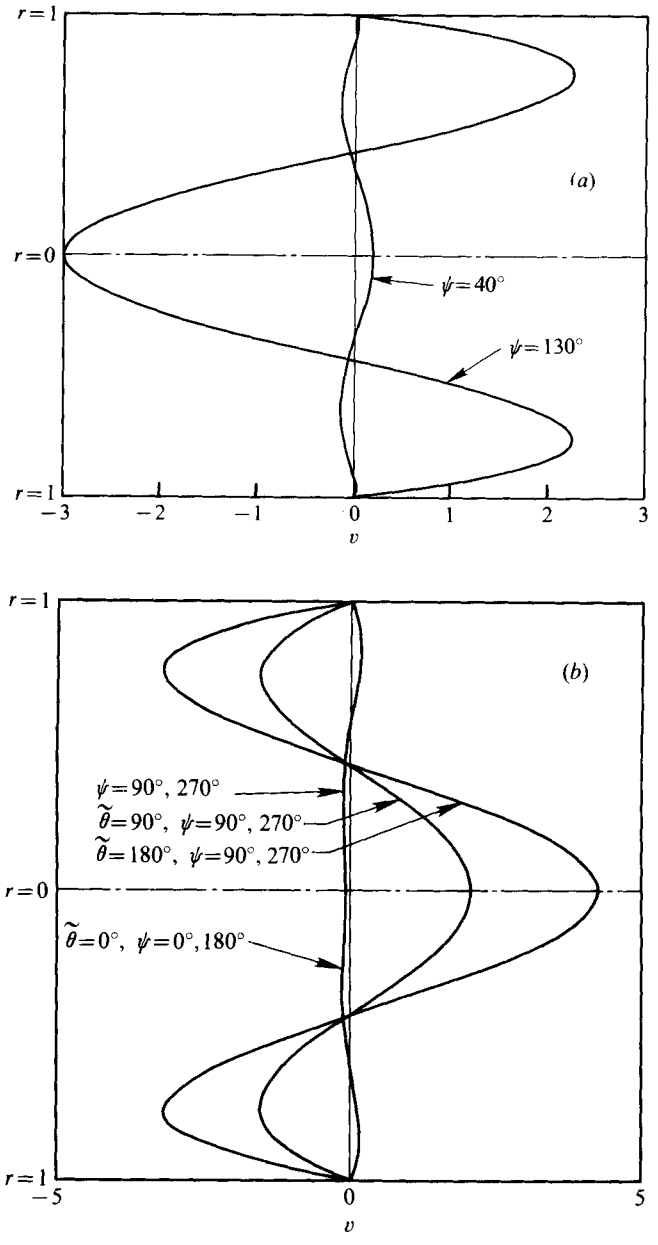

FIGURE 4. Secondary flow velocity profiles in (*a*) a horizontal and (*b*) a vertical pipe ($ReRa = 1000$, $D = 300$).

force is dominant. On the middle plane of the curved pipe ($\tilde{\theta} = 90°$), where the buoyancy force is perpendicular to the centrifugal force, the maximum velocity point is displaced towards the outside of the bend owing to the centrifugal force. At the bottom of the pipe ($\tilde{\theta} = 180°$), where the centrifugal force and the buoyancy force enhance each other, the point of maximum velocity also moves towards the outside of the bend. Physically, the distortion of the axial velocity profile is due to the displacement effect of the secondary boundary layer, as has been demonstrated by Yao (1977).

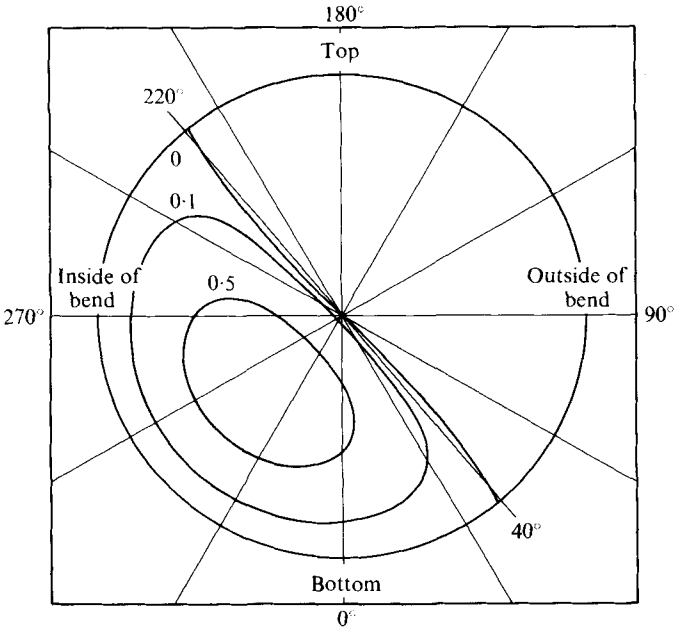

FIGURE 5. Streamlines in a horizontal curved pipe ($ReRa = 1000$, $D = 300$).

The contour of the maximum axial velocity for the vertical curved pipe is given in figure 3(*b*), which clearly shows that the line of symmetry of the two vertical vortices is 0°–180°.

Secondary flow velocity profiles and streamlines

The secondary flow velocity profiles v are presented for the horizontal curved pipe in figure 4(*a*) and for the vertical curved pipe in figure 4(*b*). For the vertical curved pipe, the secondary velocity is zero along the symmetry line (0°–180°). However, the secondary velocity does not vanish along the line 40°–220° in the horizontal curved pipe. This is because the dividing streamline is not straight. The closer the dividing streamline is to 40°–220°, the smaller is the difference between the magnitudes of the buoyancy force and the centrifugal force. The dividing streamline will be close to 0°–180° when the buoyancy force dominates; it will be close to 90°–270° when the centrifugal force is dominant. The stream functions (12*b*) and (18*b*) are plotted in figures 5 and 6. In figure 5 the skewness of the dividing streamline has been identified by comparing it with the straight line 40°–220°.

Shear stress

The axial shear stress is proportional to the value of $\partial w/\partial r$ at $r = 1$, which can be determined from (12*a*) and (18*a*). Therefore for the horizontal curved pipe

$$\tau_{r\theta} \sim \left.\frac{\partial w}{\partial r}\right|_{r=1} = -2 - \frac{ReRa}{5760}\cos\psi - \frac{D}{1920}\sin\psi. \tag{19}$$

The location of the maximum (or minimum) axial shear stress can be shown from (19) to be at

$$\psi = \tan^{-1}(3D/ReRa). \tag{20}$$

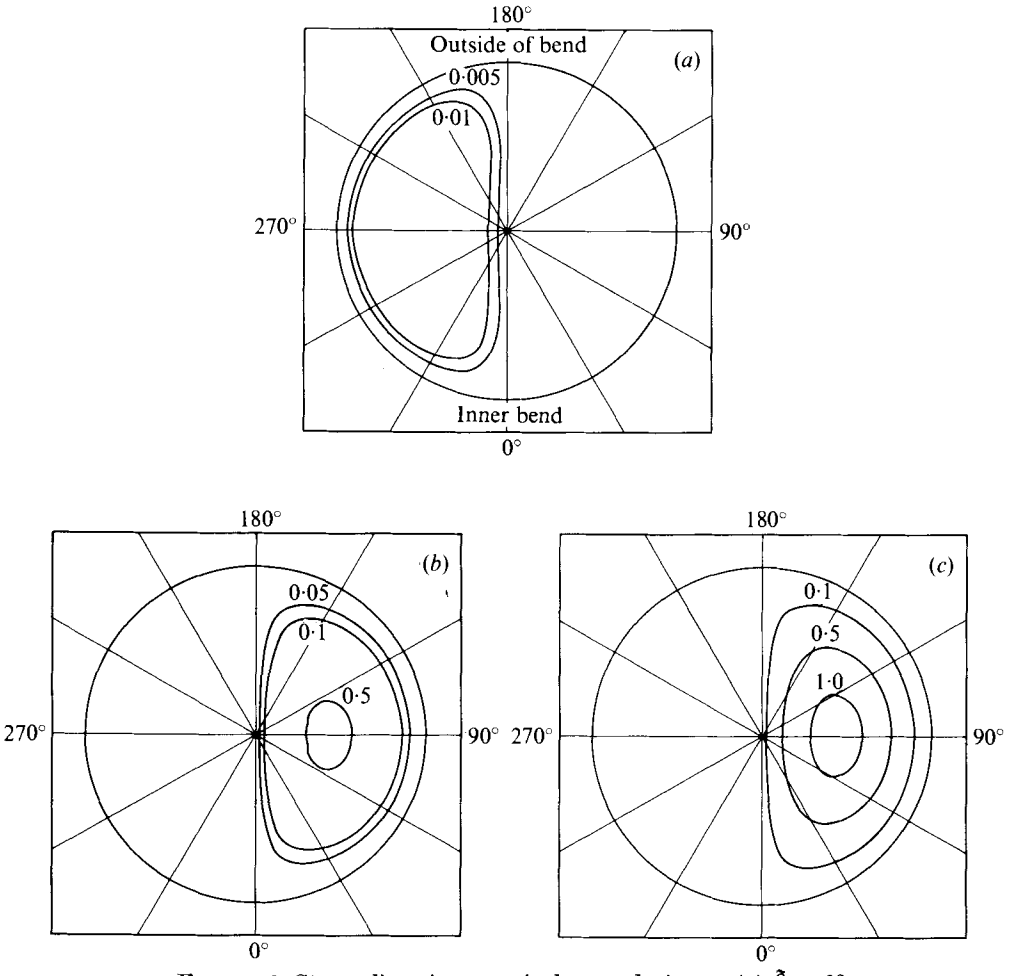

FIGURE 6. Streamlines in a vertical curved pipe at (*a*) $\tilde{\theta} = 0°$, (*b*) $\tilde{\theta} = 90°$ and (*c*) $\tilde{\theta} = 180°$ ($ReRa = 1000$, $D = 300$).

For $D = 300$ and $ReRa = 1000$, the maximum axial shear stress thus occurs at $\psi = 41{\cdot}987°$ and the minimum axial shear stress at $\psi = 221{\cdot}987°$. Similarly, the circumferential shear stress can be written as

$$\tau_{r\psi} \sim [\partial v/\partial r]_{r=1} = 0{\cdot}156[-ReRa \sin\psi + 2{\cdot}667D \cos\psi]. \tag{21}$$

Its maximum and minimum values are located at

$$\psi = \tan^{-1}(-ReRa/2{\cdot}667D), \tag{22}$$

which for $D = 300$ and $ReRa = 1000$ become $\psi = 128{\cdot}663°$ and $308{\cdot}663°$.

For the vertical curved pipe, the axial and circumferential shear stresses are

$$\tau_{r\theta} \sim -2 - \frac{\cos\psi}{5760}[ReRa \cos\tilde{\theta} - 3D] \tag{23}$$

and

$$\tau_{r\psi} \sim -0{\cdot}0156(ReRa \cos\tilde{\theta} - 2{\cdot}667D)\sin\psi. \tag{24}$$

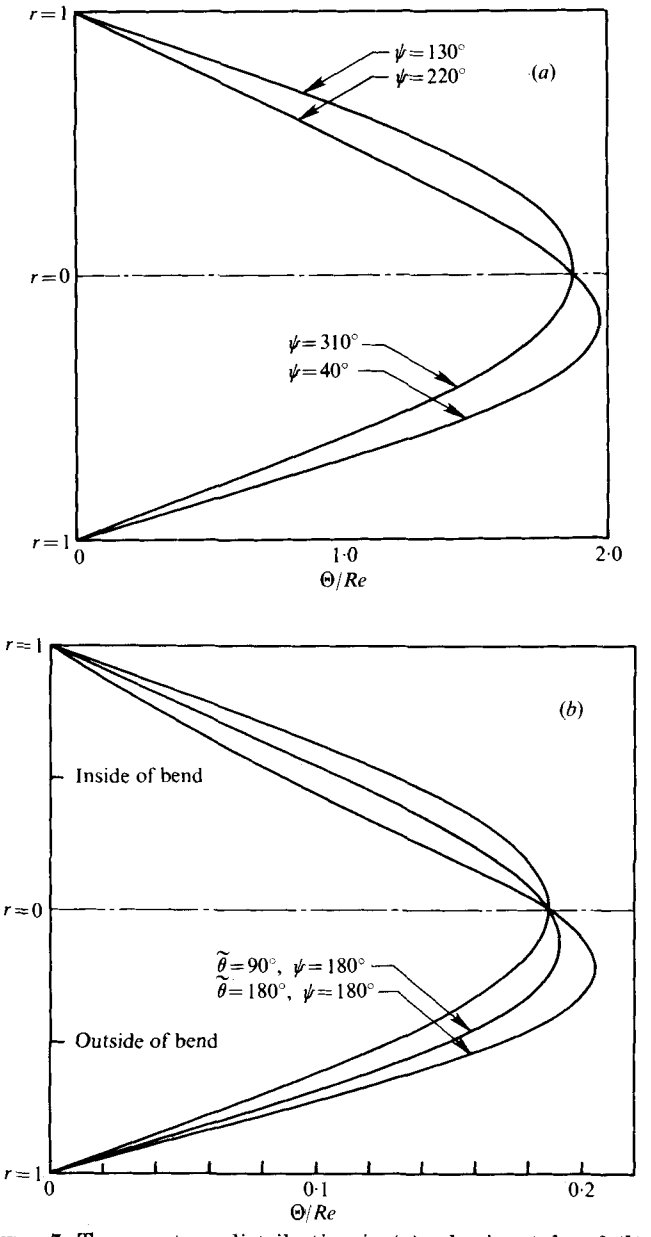

FIGURE 7. Temperature distribution in (*a*) a horizontal and (*b*) a vertical curved pipe ($ReRa = 1000$, $D = 300$, $Pr = 1$).

It is obvious that the maximum $\tau_{r\theta}$ occurs at $\tilde{\theta} = 180°$, $\psi = 0°$ and the maximum $\tau_{r\psi}$ at $\tilde{\theta} = 180°$, $\psi = \pm 90°$.

Temperature distribution and heat transfer

The fluid temperature distributions are given in figures 7 (*a*) and (*b*), for the horizontal and vertical curved pipes, respectively, and are seen to be distorted in similar ways to the axial velocity profiles.

Pr	max Nu	min Nu
0	41·987°	221·987°
0·001	42·133°	222·133°
1·0	46·371°	226·371°
10·0	47·943°	227·943°
∞	48·190°	228·190°

TABLE 1. Location of maximum and minimum Nusselt number for $D = 300$ and $ReRa = 1000$ [see (26)].

The Nusselt numbers can be determined from (12 *c*) and (18 *c*):

$$\frac{Nu_h}{Re} = -0{\cdot}25 - 0{\cdot}000013[(1+2{\cdot}615Pr)\,ReRa\cos\psi + (3+8{\cdot}05Pr)\,D\sin\psi], \quad (25\,a)$$

$$\frac{Nu_v}{Re} = -0{\cdot}25 - 0{\cdot}000013[(1+2{\cdot}615Pr)\,ReRa\cos\tilde{\theta} - (3+8{\cdot}05Pr)\,D]\cos\psi, \quad (25\,b)$$

where the subscript h denotes the horizontal curved pipe and the subscript v the vertical curved pipe. The location of the point of maximum (or minimum) heat-transfer rate for a horizontal curved pipe can be determined from (25 *a*) to be

$$\psi = \tan^{-1}\left[\frac{3+8{\cdot}05Pr}{1+2{\cdot}16Pr}\,\frac{D}{ReRa}\right]. \quad (26)$$

For fixed D and $ReRa$, the value of ψ depends only on the Prandtl number and increases slightly when the Prandtl number increases, as shown in table 1. For $Pr = 0$, the location of maximum (or minimum) heat transfer coincides with the location of maximum (or minimum) axial shear stress. For $Pr \neq 0$, these two points are slightly dislocated. For the vertical curved pipe, the maximum Nusselt number occurs at $\tilde{\theta} = 180°$, $\psi = 0°$ and the minimum Nusselt number at $\tilde{\theta} = 180°$, $\psi = 180°$.

REFERENCES

BARUA, S. N. 1963 On secondary flow in stationary curved pipes. *Quart. J. Mech. Appl. Math.* **16**, 61.

COLLINS, W. M. & DENNIS, S. C. R. 1975 The steady motion of a viscous fluid in a curved tube. *Quart. J. Mech. Appl. Math.* **28**, 133.

DEAN, W. R. 1927 Note on the motion of fluid in a curved pipe. *Phil. Mag.* **4**, 208.

DEAN, W. R. 1928 The stream-line motion of fluid in a curved pipe. *Phil. Mag.* **5**, 673.

EUSTICE, J. 1911 Flow of water in curved pipes. *Proc. Roy. Soc.* A **85**, 119.

GREENSPAN, D. 1973 Secondary flow in a curved tube. *J. Fluid Mech.* **57**, 167.

MCCONALOGUE, D. J. & SRIVASTAVA, R. S. 1968 Motion of a fluid in a curved tube. *Proc. Roy. Soc.* A **307**, 37.

MORI, Y. & NAKAYAMA, W. 1965 Study on forced convective heat transfer in curved pipes. *Int. J. Heat Mass Transfer* **8**, 67.

MORTON, B. R. 1959 Laminar convection in uniformly heated horizontal pipes at low Rayleigh numbers. *Quart. J. Mech. Appl. Math.* **12**, 410.

SINGH, M. P. 1974 Entry flow in a curved pipe. *J. Fluid Mech.* **65**, 517.

TAYLOR, G. I. 1929 The criterion for turbulence in curved pipes. *Proc. Roy. Soc.* A **124**, 243.

VAN DYKE, M. 1978 Extended Stokes series: laminar flow through a loosely coiled pipe. *J. Fluid Mech.* **86**, 129.

YAO, L. S. 1977 Entry flow in a heated straight tube. *Rand Corp. Rep.* R-2111-ARPA.

YAO, L. S. & BERGER, S. A. 1975 Entry flow in a curved pipe. *J. Fluid Mech.* **67**, 177.